IEEE Photonics Journal
An IEEE Photonics Society Publication

Open Access

Ultrasmall Mode Volumes of Multilayered Hyperbolic Metamaterial Nanocavities in the Visible Range

Volume 9, Number 5, October 2017

Song Yang
Jianhua Yang
Xiaokang Song
Yuanqi Huang
Li Yu

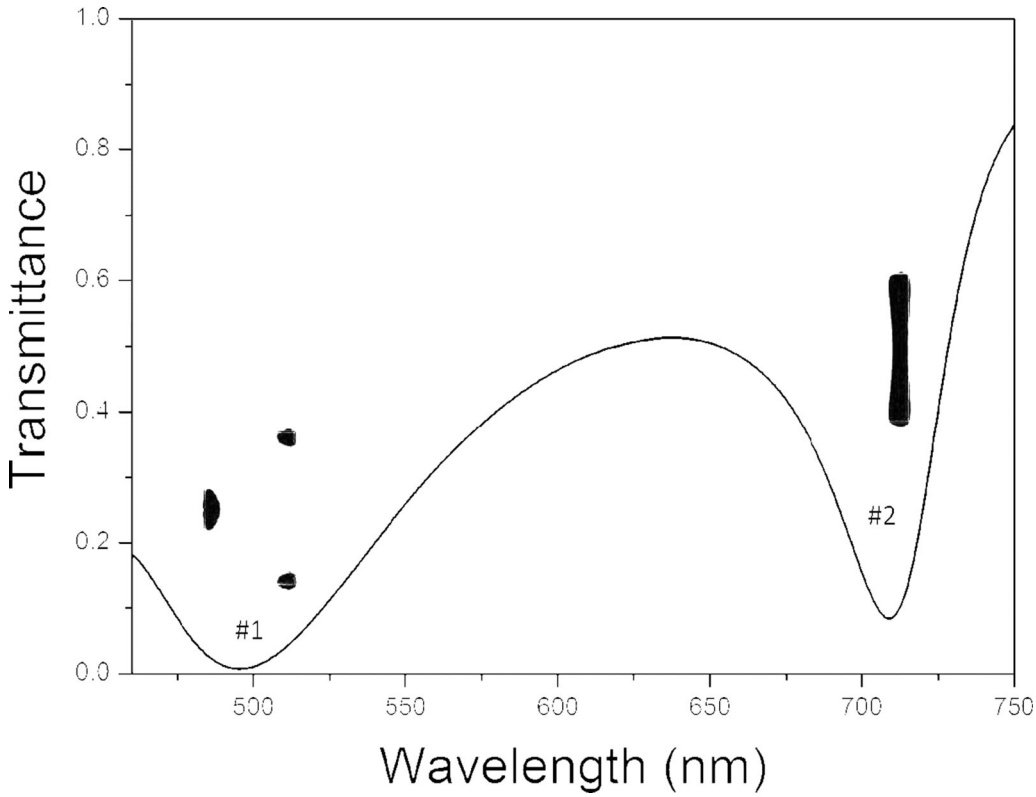

DOI: 10.1109/JPHOT.2017.2730918
1943-0655

IEEE photonics SOCIETY

IEEE

Ultrasmall Mode Volumes of Multilayered Hyperbolic Metamaterial Nanocavities in the Visible Range

Song Yang, Jianhua Yang, Xiaokang Song, Yuanqi Huang, and Li Yu

State Key Laboratory of Information Photonics and Optical Communications, Beijing University of Posts and Telecommunications, Beijing 100876, China

DOI:10.1109/JPHOT.2017.2730918

Manuscript received June 6, 2017; revised July 19, 2017; accepted July 19, 2017. Date of publication July 24, 2017; date of current version August 1, 2017. This work was supported in part by the Ministry of Science and Technology of China under Grant 2016YFA0301300, in part by the National Natural Science Foundation of China under Grants 11374041, 11574035, and 11404030, and in part by the Fund of State Key Laboratory of Information Photonics and Optical Communications, Beijing University of Posts and Telecommunications, China. Corresponding author: Li Yu (e-mail: yuliyuli@bupt.edu.cn).

Abstract: Designing optical nanocavities with high quality factors (Q) or small mode volume (Vm) has important applications in the field of quantum information due to the strong light-matter coupling phenomena. The multilayered hyperbolic metamaterial (HMM) nanocavities have been designed and numerically investigated to achieve the small mode volume. Unique dispersion relations of our HMM nanocavity enable propagation of large wave vectors result in strong wave confinement. The excitation of coupled localized surface plasmons, which have achieved ultrasmall mode volume below $10^{-6}\,\lambda^3$ or high Q/Vm around $10^7\,\lambda^{-3}$ causing better electric fields confinement. These properties can be demonstrated by rationally the geometrical parameters and may have potential applications in light-matter interaction.

Index Terms: Mode volume, quality factor, metamaterial, plasmonics.

1. Introduction

In the field of cavity quantum electrodynamics (cQED), it is highly interesting to find an optical nanocavity with ultrasmall mode volume (Vm) that could allow for many attractive strong light-matter coupling phenomena to be applied to quantum information processing and quantum communication [1], [2]. There are various types of optical nanocavities with different performances in terms of optical confinement. Dielectric cavities such as microdisks [3], [4], photonic crystals [5], [6], and metal claddings [7] work well in confining the optical field with ultrahigh Q factor. However, due to the limitation of the diffraction limit, their physical size is larger than the wavelength. This is not conducive to the realization of sub-wavelength spatial confinement. In contrast, plasmonic cavities can achieve better spatial confinement with Vm below $10^{-5}\lambda^3$ [8]–[10]. The small Vm facilitates strong coupling between quantum dots and nanocavities. More recently, hyperbolic metamaterial (HMM) formed by alternating layers of metal and dielectric has been into focus [11], [12]. With deliberately design of the periodically arranged nanostructure, specific optical properties are realized in a certain spectral range [13], [14], such as optical antenna [15], subwavelength imaging [16]–[18], cloaking [19], [20] and lasing action [21], [22]. For the HMM nanocavity, its unique dispersion relations enable propagation of large wave vectors and caused the excitation of coupled localized surface plasmons

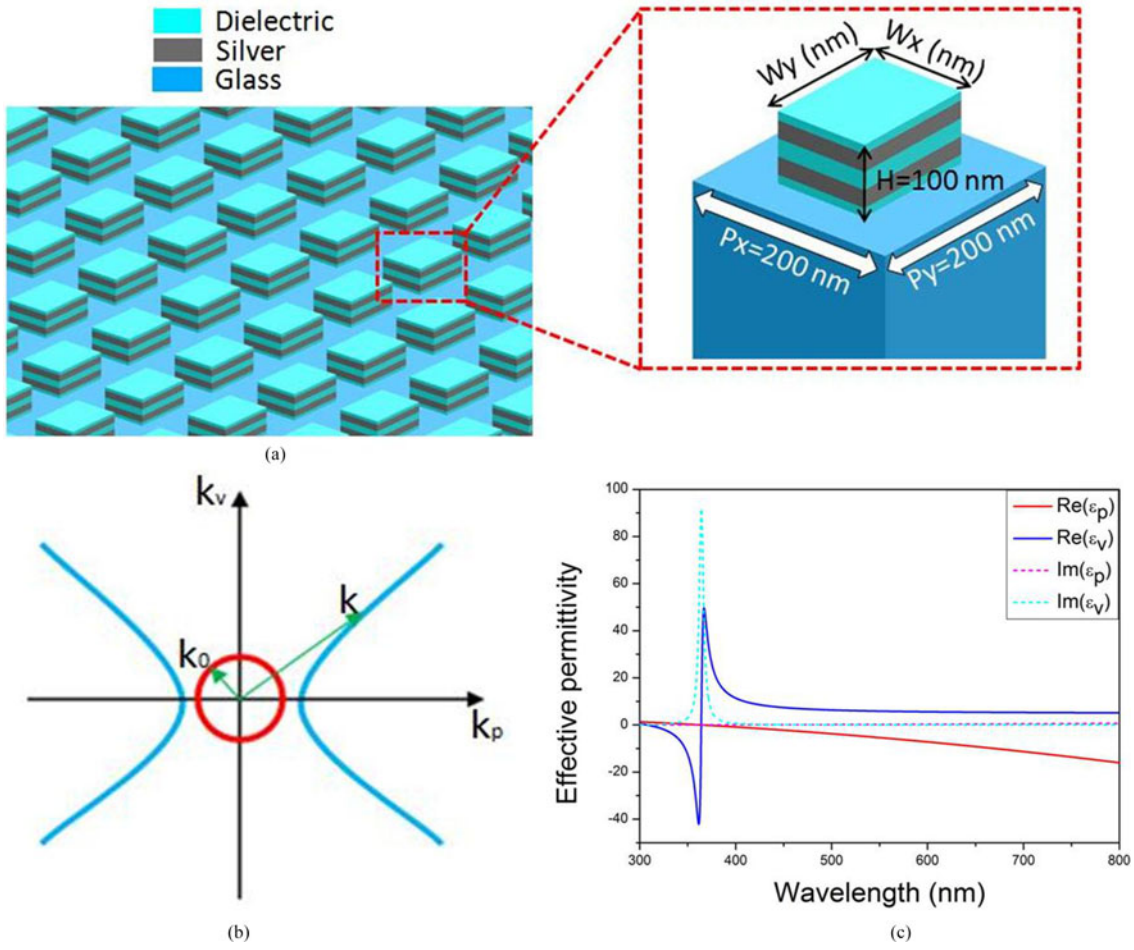

Fig. 1. (a) Schematic of multilayered nanoplate array on a glass substrate. (b) Hyperbolic Iso-frequency contour (IFC) of the multilayered HMM calculated from the dispersion relation (blue line) and the circle IFC of air with radius k_0 (red line). (c) Effective permittivities of multilayered Ag and Al_2O_3 with the metal filling ratio 0.5.

(LSPs) [23], which has achieved ultrasmall mode volume or high Q/Vm in previous works [24], [25]. However, the previous resonance wavelength is near infrared band, which is not conducive to the couple with the quantum dots in the visible range.

In this paper, we investigate optical properties in multilayered HMM nanocavity, by adjusting the geometrical size to change the position of resonance and keep the resonance wavelength in the visible range. The transmission spectrum will have two dips when the light illuminates this cavity from the glass substrate. The electric field distribution demonstrates that the two dips correspond to two different modes. And the two modes' broad spectrums are easier to implement the mode coupling between the cavity and the quantum dots. We explore the best properties of different modes under different parameters and find that the Q factor can reach 21.9, and the smallest Vm can achieve around $10^{-6}\lambda^3$ or the Q/Vm can approximately be $10^7\lambda^{-3}$ in our nanocavity, respectively.

2. Structure and Analysis

We design a rectangular nanoplate array with the multilayered structure, as shown in Fig. 1(a). This structure can be regarded as one kind of HMM nanocavity made of alternating layers of silver and dielectric (Al_2O_3). In general, the multilayered structure can be considered as an

effective uniaxial medium in the case of the geometric parameter are much smaller than the free-space wavelength of the incident electromagnetic wave [26].The miniaturization of the feature size of metamaterials towards the deep nanoscale will cause the nonlocal effect to make effective medium theory(EMT) inaccurate [27]. However, due to the thickness of our metal layer is larger than 10 nm and the dielectric layer is larger than 5 nm, the impact of nonlocal effect is unremarkable [28], [29]. EMT [30] can be used to describe the optical properties of this structure. As a uniaxial medium, the diagonal elements of the permittivity tensor are corresponding to the hyperbolic relation shown in the Fig. 1(b). We utilize EMT to determine the effective permittivities, as the following equations [31]:

$$\begin{aligned} \varepsilon_p \left(\varepsilon_{xx} = \varepsilon_{yy}\right) &= p\varepsilon_m + (1 - p)\varepsilon_d \\ \varepsilon_v \left(\varepsilon_{zz}\right) &= \frac{\varepsilon_m \varepsilon_d}{(1 - p)\varepsilon_m + p\varepsilon_d} \end{aligned} \tag{1}$$

Here p is the filling ratio of metal, ε_m and ε_d are the permittivity of metal and dielectric, respectively. In this paper, we focus on silver layers for its stability in the visible region among the noble metals. The optical properties of silver are obtained from the Drude model where $\varepsilon_m(\omega) = \varepsilon_\infty - \frac{\omega_p^2}{\omega(\omega + i\gamma)}$ with the parameters $\varepsilon_\infty = 6$, the bulk plasmon frequency $\omega_p = 1.5 \times 10^{16}$ rad/s and the collision frequency $\gamma = 7.73 \times 10^{13}$ rad/s [32]. The permittivity of dielectric is around 2.4. And we calculate the effective permittivities in Fig. 1(c) according to the above formula (1).

The hyperbolic dispersion in our structure allows large wave vectors to exist, and large wave vectors allow extremely small cavity size with the ability to sustain optical modes with volumes much smaller than the cube of their vacuum wavelength, thus achieving strong wave confinement [25].We investigate the optical properties of our multilayered structure by numerical simulations based on the finite-difference time-domain (FDTD) method. In the simulations, the dimension of rectangular plasmonic cavity is Wx = 100 nm in x-direction, Wy = 120 nm in y-direction and H = 100 nm in z-direction, with the periodicity of the lattice of $Px = Py = 200$ nm. The layer sequence from the substrate to the top is Al_2O_3/Ag/Al_2O_3/Ag/Al_2O_3 with a total thickness of 100 nm, where the top and the bottom Al_2O_3 layers both are 12.5 nm, other three layers are 25 nm. Fig. 1(c) schematically illustrates that the real part of ε_p is negative and the real part of ε_v is positive as Type II HMM [23] in the visible range. In these cases, we set wavelength from 460 nm to 750 nm and polarization along x direction as the source. Anti-Symmetric and Symmetric boundary conditions are used to mimic the periodic boundary condition. And the PML boundary condition is used in the z-direction as the light illuminates along the z axis.

3. Results and Discussion

Fig. 2(a) shows the normal transmission spectra when the light illuminates this cavity from the glass substrate. We find that two transmittance dips appearing, there is a narrow transmission valley (marked Mode #1) at the wavelength $\lambda = 495.6$ nm, while there is a broad one (marked Mode #2) at $\lambda = 709$ nm. Obviously, two modes are both resonance in the visible region. Moreover, we calculated the spectra of 20 layers model and the corresponding equivalent model with EMT, the results are show in inset of Fig. 2(a). It can be found that the result more layers model is consistent well with the result of EMT. The same resonance modes are also existent in our structure, which means that when we study the resonance modes, the equivalent model with EMT is effective for permittivity.

In order to understand the origin of these resonance modes, we calculated the electromagnetic field distributions for two modes in this cavity. To gain a complete picture of these two modes, we draw the Ez field at the y = 0 nm plane and z = 50 nm plane, respectively. Fig. 2(b) and (d) illustrate the electric field patterns for the Mode #1. This indicates that the electric field is strongly confined in the intermediate dielectric layer and our structure exhibits high energy storage capacity. For Mode #1, the resonance mode is coded index (1,3,1), according to the half-wavelength standing wave

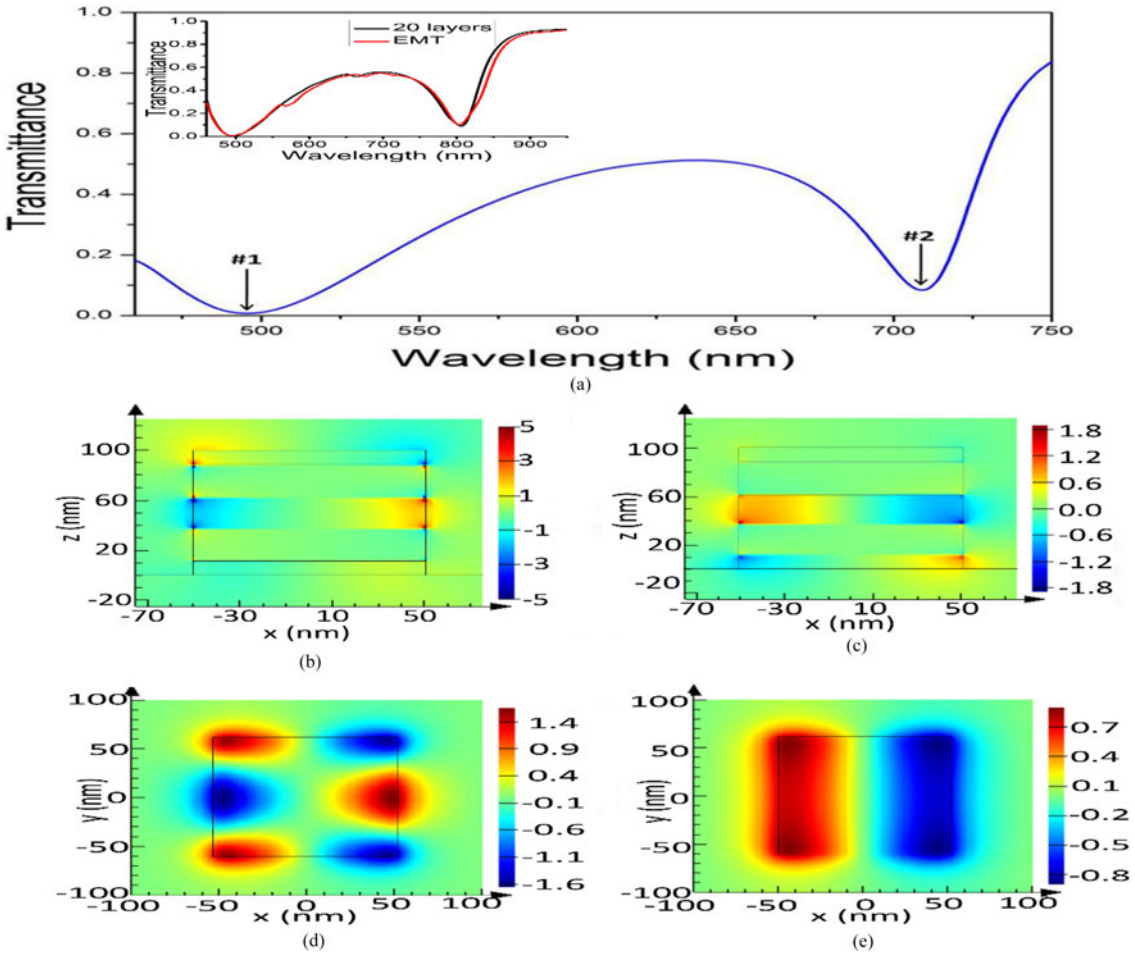

Fig. 2. (a)The calculated normal transmission spectra for the structure described in Fig. 1(a). (b)and (d) are the electric field distribution of z-component (Ez) for Mode #1 at y = 0 nm and z = 50 nm, respectively. (c) and (e) are the electric field distribution of z-component (Ez) for Mode #2 at y = 0 nm and z = 50 nm, respectively. Here, the incident light illuminates along the z-axis with x-polarization.

behaviors [33]. Fig. 2(c) and (e) illustrate the electric field distributions of Mode #2. A similar analysis shows that the resonance order is (1,1,1) of Mode #2. The electric field distributions show that the two resonances originate from the coupling of LSPs [34], and our structure can be considered as a plasmonic nanocavity. Compared with other multilayered structure [35], there are more energy local in the cavity and less electric field at the corner, hence our structure's energy storage capacity is better.

Two vital parameters, the quality factor (Q factor) and mode volume (Vm), can be used to characterize the energy storage capacity of optical nanocavities [36]. For the certain resonance mode, the Q factor is determined by the photon life time. In our simulation work, we can use $Q = f_R/\Delta f$ to compute the Q factor, where f_R is the resonant frequency and Δf is the full width half maximum (FWHM) of the resonant dips. We calculate the Q factor of two modes and they are 3.7 for Mode #1 and 12.4 for Mode #2, respectively. Although these results are better than the previous work [24], our cavity's Q factors are much lower than the dielectric optical cavities work [37]. Due to all metal-dielectric nanocavity exists nonnegligible metal loss,which restricts the Q factor [28].

However, plasmonic cavities can achieve better spatial confinement [9], [10]. The Vm is an effective volume when modes are distributed at the peak intensity [38].Our cavity has smaller Vm

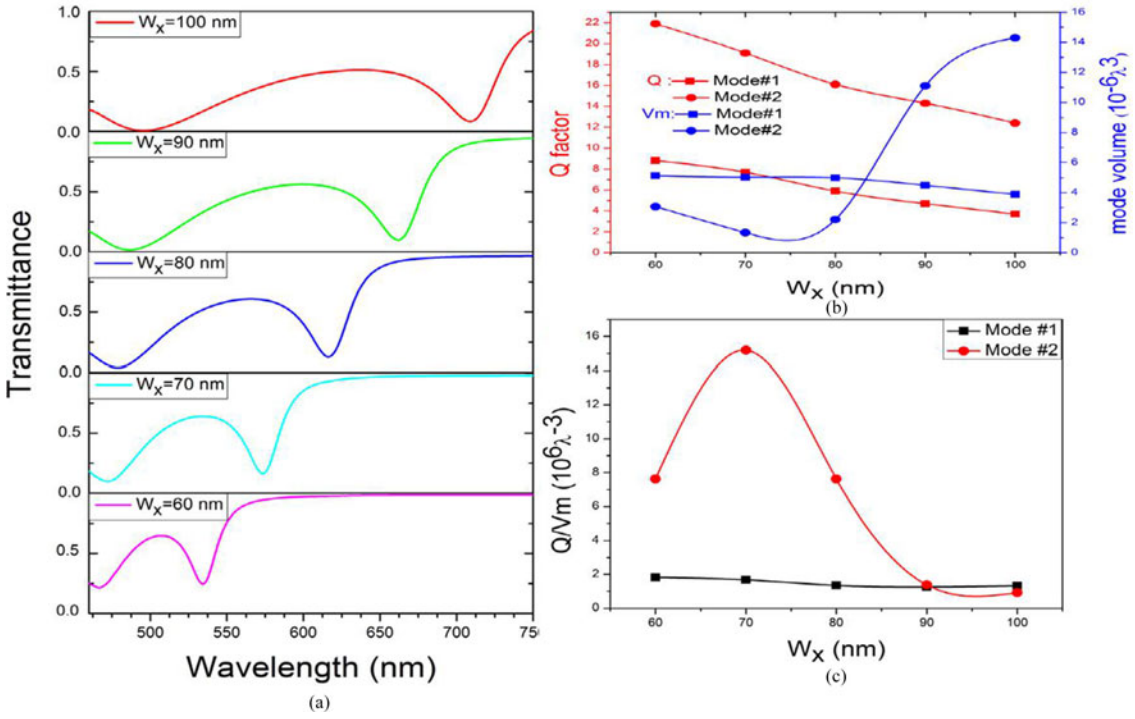

Fig. 3. (a) The calculated normal transmission spectra of multilayered nanocavities with varying the width Wx from 60 nm to 100 nm. (b) Q factor and Vm of multilayered nanocavities as functions of Wx for two modes. (c) Q/Vm as functions of Wx for two modes.

compared to dielectric cavities [39].The Vm is calculated by [25], [33]:

$$Vm = \frac{1}{\max\left(\varepsilon(\vec{r})\left|\vec{E}(\vec{r})\right|^2\right)} \iiint \varepsilon(\vec{r})\left|\vec{E}(\vec{r})\right|^2 d^3\vec{r} \tag{2}$$

where $\varepsilon(\vec{r})$ is the dielectric permittivity and $\vec{E}(\vec{r})$ is electric field at the spatial location $\vec{r}$. All of our structure is chosen to calculate the maximum energy density by FDTD method. Our calculations reveal that the Vm can go down to $2.79 \times 10^{-6}\lambda^3$ for Mode #1 and $1.34 \times 10^{-5}\lambda^3$ for Mode #2. The Vms are small than the results in previous work [24] as our expectation, which reveals that our structure is reasonable. The ultrasmall results prove that our cavity can confine electromagnetic energy far below the diffraction limit and may have potential applications in light-matter interaction.

In order to improve the performance of our cavity, we need to further explore the factors that affect the optical properties. Our multilayered plasmonic cavity can be regarded as a three-dimensional subwavelength resonator formed by HMM [40].This kind of cavity allows propagation of large momentum waves (Fig. 1(b)) and introduces a strong mode mismatch between the cavity and the air background which results in total internal reflection (TIR).Our structure can be considered as a cavity couping of LSPs due to the TIR feedback mechanism [35].Therefore, we can adjust the geometrical parameters to change the optical properties to obtain the best results.

Firstly, we only adjust the width of this cavity along the x direction (Wx) and keep other geometry parameters. Fig. 3(a) shows the transmission spectra for the Wx from 100 nm to 50 nm. As the Wx shrinks, the resonance position of both Mode #1 and Mode #2 shit to the blue obviously. This phenomenon illustrates that the resonance position depends on the Wx which along the polarization direction. So that we can adjust the Wx and change the resonance wavelength to realize the interaction between our cavity and the quantum dots with different wavelengths.

The different optical transmittance in our spectra might influence the properties of our cavity. So we calculat the Q factor and Vm for each of cavities. In the Fig. 3(b), the red lines represent the

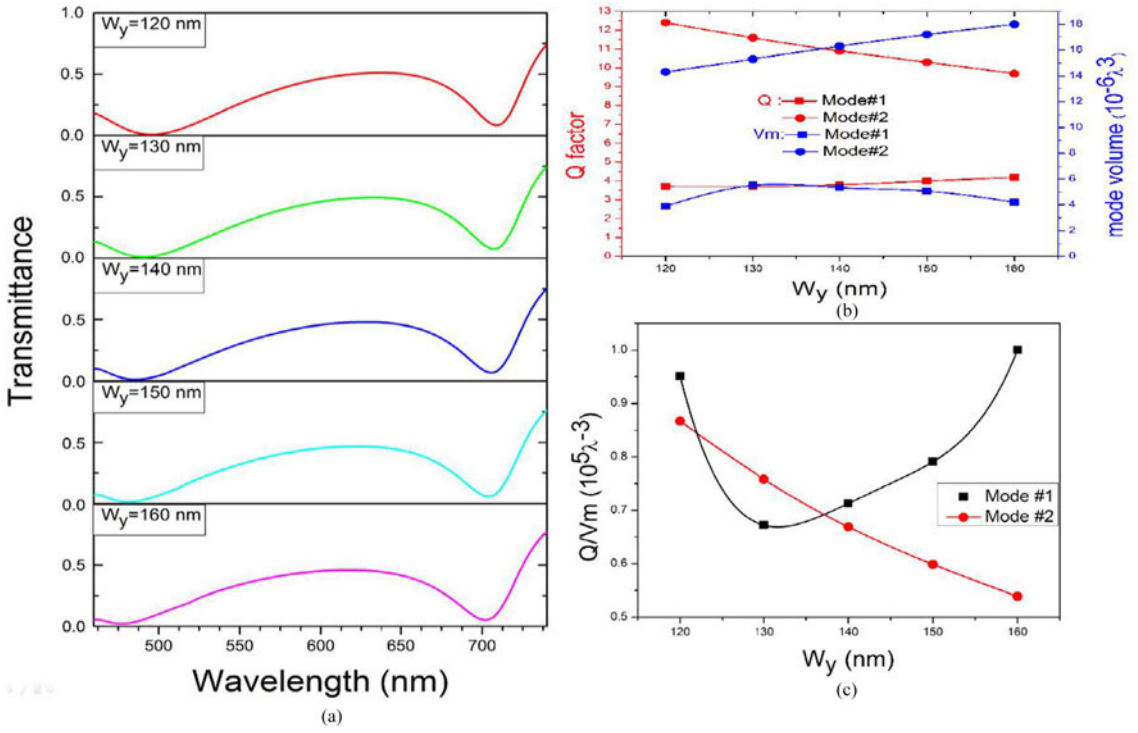

Fig. 4. (a) The calculated normal transmission spectra of multilayered nanocavities with varying the width Wy from 120 nm to 160 nm. (b) Q factor and Vm of multilayered nanocavitiesas functions of Wy for two modes. (c) Q/Vm as functions of Wy for two modes.

Q factor and the square and circular represents the Mode #1 and Mode #2, respectively. Fig. 3(b) shows that the Q factor of Mode #2 is higher than Mode #1 and illustrates that the lower order optical mode have higher Q factor in our cavities. Corresponding to Fig. 3(a), the transmission valley of Mode #2 is narrower than Mode #1 for each cavity with different Wx, which makes the higher Q factor for Mode #2. For each optical mode, Q factor is decrease with the increase of Wx, which corresponds with the broader valley in Fig. 3(a). This HMM cavity's anomalous phenomenon between Q factor and geometry had been mentioned in previous work [33]. The Q factor can reach 21.9 when the Wx is only 60 nm as the shortest Wx. Then, we focus on the blue lines in the Fig. 3(b) which represents the Vm of our cavity. We notice that the trend of the two lines is different. The main reason for this phenomenon is the different field distribution between two modes. And the smallest Vm reach $1.26 \times 10^{-6}\lambda^3$ when the Wx at 70 nm. The combination of Q factor and Vm, the Purcell factor, is proportional to the Q/Vm and is another main property for optical cavity. The lower order mode has smaller Vm due to the filed distribution [24], [41] and higher Q factor due to the absorption of metal [42], so that it will have higher Q/Vm ratio and higher optical confinement comparing with the higher order mode. We calculate the Q/Vm for two modes and add them into the Fig. 3(c). In the Fig. 3(c), the black line of Mode #1 always keep a smaller value about $10^6\lambda^3$, the red line of Mode #2 exist a peak about $1.52 \times 10^7\lambda^3$ which approach the result of previous work [36].

Subsequently, we adjust the width of this cavity along the y direction(Wy) and keep other geometry parameters. Fig. 4(a) shows the transmission spectra for the Wy from 120 nm to 160 nm. As the Wy increase, the resonance position of both Mode #1 and #2 shift to the blue unobviously. The changes of width and depth of these valleys are small, so their Q factors change lightly in Fig. 4(b). Although the biggest Q factor is 12.4 when we keep the former size, is still smaller than the result in Fig. 3(b). It is shown that the Q factor can be obtained by adjusting the length of the cavity along the direction of polarization, which is higher than that of adjusting the vertical polarization direction.The

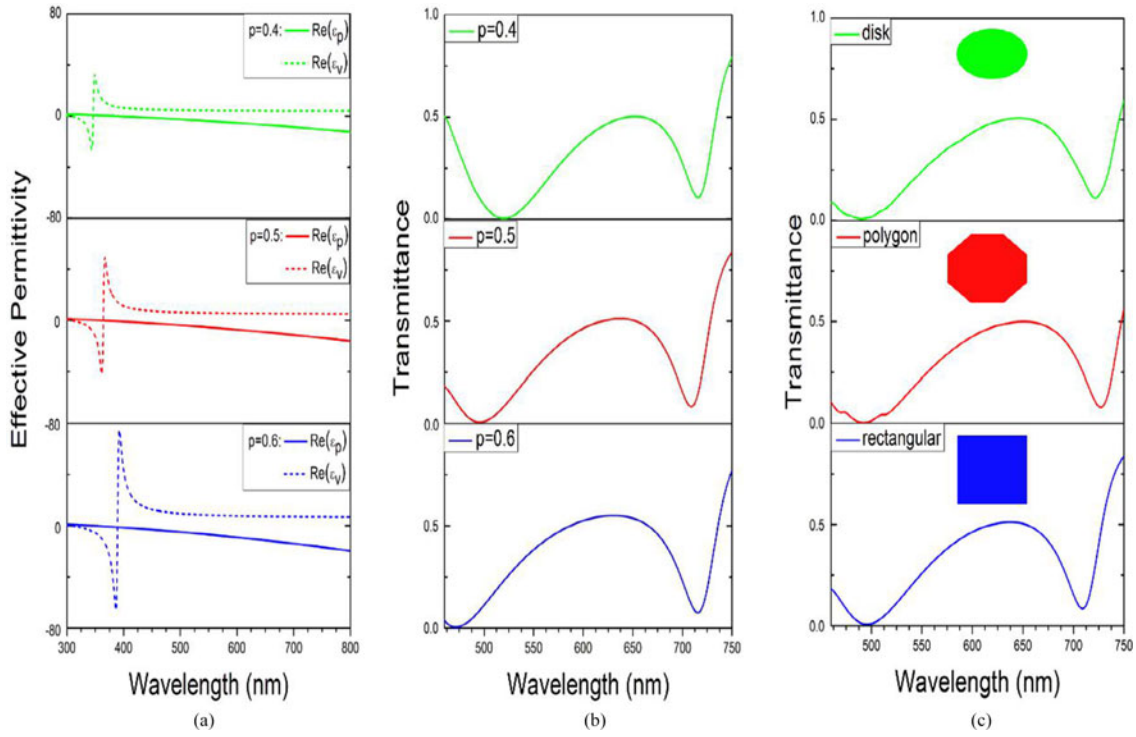

Fig. 5. (a) The real part of εp and εv for multilayered nanocavities with three different filling ratios p. (b) The calculated normal transmission spectra of multilayered nanocavities with p from 0.4 to 0.6. (c) The calculated normal transmission spectra of three different shape of the optical cavity: rectangular, polygon and disk.

same is true for other parameters. The smallest Vm is 3.89 $\times$ $10^{-6}\lambda^3$ when the Wy at 120 nm for Mode #1,which is bigger than result mentioned above. And the magnitude of the Q/Vm in Fig. 4(c) is $10^5\lambda^{-3}$ smaller than the mentioned above. So we can safely draw the conclusion that the optical properties of adjusting the geometric parameter along the polarization direction are better than that perpendicular to the polarization direction.

Finally, as a HMM optical cavity, we can change the filling ratio of metal (p) to change the effective permittivities. Fig. 5(a) depicts the real part of ε_p and ε_v of multilayer structure for the filling ratios p $=$ 0.4 to p $=$ 0.6. With the change of p, the real part of ε_v have changed significantly and ε_p still less than zero in the visible range. This guarantees that within the range of our discussion, the dispersion relation is always hyperbolic, though the p has changed a little. In Fig. 5(b), resonant position of the cavity remains in the visible range, ensuring that the resonance position will not be much deviation as the metal ratio generates insignificant errors in experiment. In Fig. 5(c), there are two similar modes in each transmission spectrum for cavity with different shapes (keep the same area): rectangular, polygon and disk. Two distinct dips only have a slight shift for different shapes, which indicate that the main resonant modes determined by the LSPs which rely on the configuration of the multilayer films. And the slight fluctuations in the spectra illustrates that the shape of the cross-section has little influence. While ensuring the cavity of the adjustable and stability.

4. Conclusion

In conclusion, we have investigated the optical properties of multilayered plasmonic nanocavity with deep subwavelength size in all three dimensions by numerical simulations. The hyperbolic dispersion allows to a large momentum wave and LSPs cause the Vm much smaller than the

vacuum wavelength. The properties of these cavities, can be tuned by the geometrical parameters, such as resonance wavelength, Q factor and Vm. As the result, the optical properties of adjusting the geometric parameter along the polarization direction are better than that perpendicular to the polarization direction. The Q factor can reach 21.9, the smallest Vm is around $10^{-6}\lambda^3$ and the Q/Vm is about $10^{7}\lambda^{-3}$. Under some conditions, the deviation of these properties is very small with the changes of size and refractive index, which is conducive to maintaining the stability of the cavity. These unique properties of multilayered cavity increase the optical density of states and therefore could be applied to light-matter interactions, such as cavity quantum electrodynamics, luminescence enhancement and quantum information processing.

References

[1] A. Wallraff *et al.*, "Strong coupling of a single photon to a superconducting qubit using circuit quantum electrodynamics," *Nature*, vol. 431, no. 7005, pp. 162–167, 2004.
[2] P. Lodahl, S. Mahmoodian, and S. Stobbe, "Interfacing single photons and single quantum dots with photonic nanostructures," *Rev. Modern Phys.*, vol. 87, no. 2, pp. 347–400, 2015.
[3] R. D. Schilling, H. Schütz, A. Ghadimi, V. Sudhir, D. Wilson, and T. Kippenberg, "Near-field integration of a si3n4 nanobeam and a sio2 microcavity for Heisenberg-limited displacement sensing," *Phys. Rev. Appl.*, vol. 5, 2016, Art. no. 054019.
[4] M. Mitchell, A. C. Hryciw, and P. E. Barclay, "Cavity optomechanics in gallium phosphide microdisks," *Appl. Phys. Lett.*, vol. 104, no. 14, 2014, Art. no. 141104.
[5] H. Sekoguchi, Y. Takahashi, T. Asano, and S. Noda, "Photonic crystal nanocavity with a q-factor of ~9 million," *Opt. Exp.*, vol. 22, no. 1, pp. 916–924, 2014.
[6] A. Bazin, R. Raj, and F. Raineri, "Design of silica encapsulated high-q photonic crystal nanobeam cavity," *J. Lightw. Technol.*, vol. 32, no. 5, pp. 952–958, Mar. 2014.
[7] M. Nami and D. F. Feezell, "Optical properties of plasmonic light-emitting diodes based on flip-chip iii-nitride core-shell nanowires," *Opt. Exp.*, vol. 22, no. 24, pp. 29445–29455, 2014.
[8] Z. Yu, Z. Gao, Z. Song, and Z. Wang, "Terahertz spoof plasmonic coaxial microcavity," *Appl. Opt.*, vol. 53, no. 6, pp. 1118–1123, 2014.
[9] L. Jaehak, S. Sangkeun, C. Jun-Hyuk, E. S. Chan, M. N. Asger, and J. H. Shin, "Ultra sub-wavelength surface Plasmon confinement using air-gap, sub-wavelength ring resonator arrays," *Sci. Rep.*, vol. 6, 2016, Art. no. 22305.
[10] Z. Li, J. L. Kou, M. Kim, J. O. Lee, and H. Choo, "Highly efficient and tailorable on-chip metal–insulator–metal plasmonic nanofocusing cavity," *ACS Photon.*, vol. 1, no. 10, pp. 944–953, 2014.
[11] I. I. Smolyaninov, "Hyperbolic metamaterials," *Nature Photon.*, vol. 7, no. 12, pp. 948–957, 2015.
[12] P. Shekhar, J. Atkinson, and Z. Jacob, "Hyperbolic metamaterials: Fundamentals and applications," *Nano Convergence*, vol. 1, no. 1, 2014, Art. no. 14.
[13] V. M. Shalaev, "Optical negative-index metamaterials," *Nature Photon.*, vol. 1, no. 1, pp. 41–48, 2007.
[14] C. M. Soukoulis and M. Wegener, "Past achievements and future challenges in the development of three-dimensional photonic metamaterials," *Nature Photon.*, vol. 5, no. 9, pp. 523–530, 2011.
[15] P. Biagioni, J. S. Huang, and B. Hecht, "Nanoantennas for visible and infrared radiation," *Rep. Progress Phys. Phys. Soc.*, vol. 75, no. 2, 2012, Art. no. 024402.
[16] T. Xu, A. Agrawal, M. Abashin, K. J. Chau, and H. J. Lezec, "All-angle negative refraction and active flat lensing of ultraviolet light," *Nature*, vol. 497, no. 7450, pp. 470–474, 2013.
[17] X. Zhang and Z. Liu, "Superlenses to overcome the diffraction limit," *Nature Mater.*, vol. 7, no. 6, pp. 435–441, 2008.
[18] J. Sun, M. I. Shalaev, and N. M. Litchinitser, "Experimental demonstration of a non-resonant hyperlens in the visible spectral range," *Nature Commun.*, vol. 6, 2015, Art. no. 7201.
[19] N. Landy and D. R. Smith, "A full-parameter unidirectional metamaterial cloak for microwaves," *Nature Mater.*, vol. 12, no. 1, pp. 25–28, 2013.
[20] Z. J. Wong, X. Ni, M. Mrejen, Y. Wang, and X. Zhang, "An ultrathin invisibility skin cloak for visible light," *Science*, vol. 349, no. 6254, pp. 1310–1314, 2015.
[21] R. Chandrasekar *et al.*, "Lasing action with gold nanorod hyperbolic metamaterials," *ACS Photon.*, vol. 4, no. 3, pp. 674–680, 2017.
[22] Z. Wang *et al.*, "Controlling random lasing with three-dimensional plasmonic nanorod metamaterials," *Nano Lett.*, vol. 16, no. 4, pp. 2471–2477, 2016.
[23] L. Ferrari, C. Wu, D. Lepage, X. Zhang, and Z. Liu, "Hyperbolic metamaterials and their applications," *Progress Quantum Electron.*, vol. 40, pp. 1–40, 2015.
[24] W. T. Chen *et al.*, "Fabrication of three-dimensional plasmonic cavity by femtosecond laser-induced forward transfer," *Opt. Exp.*, vol. 21, no. 1, pp. 618–625, 2013.
[25] J. Yao, X. Yang, X. Yin, G. Bartal, and X. Zhang, "Three-dimensional nanometer-scale optical cavities of indefinite medium," *Proc. Nat. Acad. Sci. USA*, vol. 108, no. 28, pp. 11327–11331, 2011.
[26] J. Elser, R. Wangberg, V. A. Podolskiy, and E. E. Narimanov, "Nanowire metamaterials with extreme optical anisotropy," *Appl. Phys. Lett.*, vol. 89, no. 26, 2006, Art. no. 261102.
[27] W. Yan, N. A. Mortensen, and M. Wubs, "Hyperbolic metamaterial lens with hydrodynamic nonlocal response," *Opt. Exp.*, vol. 21, no. 12, pp. 15026–15036, 2013.
[28] R. Ruppin, "Non-local optics of the near field lens," *J. Phys. Condensed Matter*, vol. 17, no. 12, pp. 1803–1810, 2005.

[29] A. Moreau, C. Ciraci, and D. R. Smith, "Impact of nonlocal response on metallodielectric multilayers and optical patch antennas," *Phys. Rev. B*, vol. 87, no. 4, 2013, Art. no. 045401.
[30] Y. Liu, G. Bartal, and X. Zhang, "All-angle negative refraction and imaging in a bulk medium made of metallic nanowires in the visible region," *Opt. Exp.*, vol. 16, no. 20, pp. 15439–15448, 2008.
[31] C. A. Foss Jr., G. L. Hornyak, J. A. Stockert, and C. R. Martin, "Template-synthesized nanoscopic gold particles: optical spectra and the effects of particle size and shape," *J. Phys. Chem.*, vol. 98, no. 11, pp. 2963–2971, 1994.
[32] Z. Jacob, L. V. Alekseyev, and E. Narimanov, "Optical hyperlens: Far-field imaging beyond the diffraction limit," *Opt. Exp.*, vol. 14, no. 18, pp. 8247–8256, 2006.
[33] X. Yang, J. Yao, J. Rho, X. Yin, and X. Zhang, "Experimental realization of three-dimensional indefinite cavities at the nanoscale with anomalous scaling laws," *Nature Photon.*, vol. 6, no. 7, pp. 450–454, 2012.
[34] Y. J. Bao *et al.*, "Role of interference between localized and propagating surface waves on the extraordinary optical transmission through a subwavelength-aperture array," *Phys. Rev. Lett.*, vol. 101, no. 8, 2008, Art. no. 087401.
[35] L. Qin *et al.*, "Exchange of electric and magnetic resonances in multilayered metal/dielectric nanoplates," *Opt. Exp.*, vol. 19, no. 23, pp. 22942–22949, 2011.
[36] S. Huang *et al.*, "Ultrasmall mode volumes in plasmonic cavities of nanoparticle-on-mirror structures," *Small*, vol. 12, no. 37, pp. 5190–5199, 2016.
[37] T. Yoshie, L. Tang, and S. Y. Su, "Optical microcavity: Sensing down to single molecules and atoms," *Sensors*, vol. 11, no. 2, pp. 1972–1991, 2011.
[38] K. J. Vahala, "Optical microcavities," *Nature*, vol. 424, no. 6950, pp. 839–846, 2003.
[39] J. T. Robinson, C. Manolatou, L. Chen, and M. Lipson, "Ultrasmall mode volumes in dielectric optical microcavities," *Phys. Rev. Lett.*, vol. 95, no. 14, 2005, Art. no. 143901.
[40] Z. Huang and E. E. Narimanov, "Zeroth-order transmission resonance in hyperbolic metamaterials," *Opt. Exp.*, vol. 21, no. 12, pp. 15020–15025, 2013.
[41] F. Lou, M. Yan, L. Thylen, M. Qiu, and L. Wosinski, "Whispering gallery mode nanodisk resonator based on layered metal-dielectric waveguide," *Opt. Exp.*, vol. 22, no. 7, pp. 8490–8502, 2014.
[42] S. Tang, Y. Fang, Z. Liu, L. Zhou, and Y. Mei, "Tubular optical microcavities of indefinite medium for sensitive liquid refractometers," *Lab Chip*, vol. 16, no. 1, pp. 182–187, 2016.